Sensors and Actuators A 290 (2019) 198–206

Contents lists available at ScienceDirect

Sensors and Actuators A: Physical

journal homepage: www.elsevier.com/locate/sna

Thermal phenomena in LTCC sensor structures

Marina Santo Zarnik*, Franc Novak, Gregor Papa

Jožef Stefan Institute, Jamova cesta 39, 1000 Ljubljana, Slovenia

ARTICLE INFO

Article history:
Received 14 December 2018
Received in revised form 6 February 2019
Accepted 24 February 2019
Available online 20 March 2019

Keywords:
Temperature-dependent response
Evaporative cooling
Finite-element analysis

ABSTRACT

LTCC sensors can be used in harsh environments, but caution is needed if the measured medium or environment changes dynamically. In most cases, replacement of the medium in direct contact with the sensing structure can critically affect the sensor's response. In the case of diaphragm-type pressure sensors, problems can also arise with a non-homogeneous medium (gases with droplets of liquid or liquids with bubbles). We investigated a situation where droplets of different liquids appear on the diaphragm of a common, thick-film, piezoresistive, pressure-sensor configuration. Experiments with volatile liquids indicate that the sensor's time response depends on the dynamic changes in the temperature distribution. Furthermore, we built a simplified finite-element (FE) model in which the heat-transfer coefficient of the evaporating liquid film is defined by a time-dependent function. The simulations showed the same trends as the experimental measurements, which confirmed the assumed manifestation of the thermal phenomena. The presented work opens up new possibilities for the application of LTCC sensors.

1. Introduction

Low-temperature co-fired ceramic (LTCC), based on the lamination and sintering of green glass-ceramic tapes, is a well-established technology for reliable interconnections in electronics. Because of its desirable physical, electrical and chemical properties, coupled with an excellent capability for 3D structuring and the scalable manufacturing of different functional components, LTCC is a competitive material for micro/meso-system technology [1]. Among the most frequently discussed LTCC-based microsystems are different sensors for mechanical quantities [2–5], chemical sensors [6], sensors for biological measurements [7,8], different fluidic systems [9] and many others. The relatively low thermal conductivity of LTCC (typically about 3 W/m/K) enables the implementation of functional structures that feature regions with local high-temperature gradients such as a fluid structure with heaters in a flow sensor [4], the differential scanning calorimeter [10], and various chemical processors. As is evident from the above-mentioned studies, the advantage of LTCC lies not only in benefiting from the effective structuring, but more importantly from exploiting the specific material properties, which enable the creation of structures/systems with the many useful functionalities. However, when designing new applications, it is also necessary to take into account the specifics that can adversely influence the performance of LTCC-based devices. In this regard, we focused on pressure sensors, where possible changes or replacements with respect to the measured media might have a significant impact on their characteristics.

In our previous investigations of the influence of humid environments and assessments of LTCC sensors for use in wet-wet applications [11], we encountered a specific response of the sensor when exposed to water droplets [12]. In the present work, we analysed the physical background of the effect and developed a finite-element (FE) model of an LTCC pressure sensor to study the thermal phenomena in such physical situations. Our experiments showed that the specific sensor's time response results from the dynamic changes in the temperature distribution in the sensing structure due to the Joule heating of the resistors and the simultaneous cooling due to evaporation of the liquid on its surface. Accordingly, we defined the heat transfer of the liquids using prescribed, time-dependent, forced-convection coefficients. The simulations showed the same trends as the experimental measurements, which confirmed our modelling assumptions. The results presented in this paper could lead to new applications in real-time environmental monitoring, such as the detection/identification of drops of liquids, fluid temperature, different lab-on-a-chip devices, etc.

2. Experimental observations

2.1. Structure of the pressure sensor

The initial experimental analyses [11] were carried out on a sensor structure made of DuPont 951 green tape, the conductor DuPont 7484 (Pd/Ag) and the thick-film resistor material DuPont

* Corresponding author.
E-mail address: marina.santo@ijs.si (M.S. Zarnik).

https://doi.org/10.1016/j.sna.2019.02.031

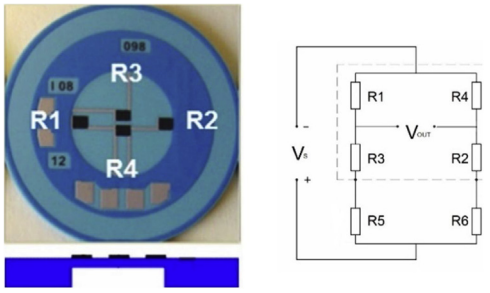

Fig. 1. LTCC-based pressure sensor with a 100-μm-thick diaphragm and a diameter of 9.6 mm, viewed from the front, and its schematic cross-section, not to scale (left), and the electrical connection (right).

2041. It actually consists of just a 3D structured, sensing diaphragm with the thick-film resistors in a full Wheatstone-bridge configuration (Fig. 1) and is open at the back to provide easy access for the controlled dropping of different liquids directly onto the sensing diaphragm. The resistors R5 and R6, which are there to balance the bridge, are placed near the border of the sensing diaphragm and protected with an ESL 240B coating. The typical sensitivity (S) of sensors with such a sensing diaphragm and with a closed pressure cavity (measured in the air) is about 14 μV/mbar, and the temperature dependence of sensitivity (TCS), in the temperature range from -25 °C to 75 °C, is 500 × 10^{-6}/°C. The offset voltage (V_{off}) of the balanced sensor at the supply voltage (V_s) of 5 V is within a few tenths of a μV, and its temperature dependence is typically 20 μV/K. The fact is, however, that the replacement or any change in the environment and/or the pressure medium can affect the above-mentioned characteristics. As shown in the following sections, the offset is particularly affected, while the sensitivity does not change critically. For the selected medium, the sensor can be calibrated accordingly and such changes, in general, are not considered to be a problem. However, they need to be understood and controlled.

2.2. Response to the changes in the medium/environment

From the point of view of the sensor's accuracy, any accidental/uncontrolled changes in the medium/environment can be problematic, since they can result in a sensor response that could be misinterpreted. Such a problematic situation occurs, for example, when drops of liquid suddenly appear on the diaphragm. In order to take a closer look at the specific situation, we further expanded the experiment described in [12], which is summarized below.

The drops of water were dispensed onto the sensing diaphragm and left there to evaporate until the surface was not completely dried (Fig. 2a). Meanwhile, we measured the output voltage (V_{out}) every 5 s, starting from the time when the sensor warmed up and stabilized in the ambient conditions of the room (i.e., about 60 min after connecting the sensor to the supply voltage, V_s, of 5 V). After a few minutes of measuring the stable response, drops of water (with a volume of about 8 μl) were dispensed, one by one, onto the middle of the diaphragm. After applying 3–5 drops, their cumulative volume was large enough to spill over the whole diaphragm. The measured sensor response ($\Delta V_{out} = V_{out} - V_{out\text{-}stab}$) is shown in Fig. 2b. The characteristic points are as follows: (1) the initial stabilized response; (2) the moment when the first drop of water touched the diaphragm, resulting in an immediate peak; (3) the drops accumulated on the central region of the diaphragm; (4) the water spreading over the entire membrane; (5) the central part of the diaphragm is already dried; (6) the narrow region at the edge of the diaphragm is wet; and (7) the stabilized response of the dried sensor. Due to cooling of the edge resistors while the central resistors start to warm, in the interval (5)–(6) the V_{out} falls, and for a short time remains even below the initial stabilized value. Furthermore, notice that the mass of the liquid drops is too small to cause the observed changes in V_{out} as a result of the mechanical load. Since the ambient conditions (temperature and pressure) are constant, a possible cause of such a response (Fig. 2b) could be the dynamic change in the temperature distribution due to the Joule heating of the thick-film resistors and the local heat dissipation due to the evaporation of the liquid. The sensor's response strongly depends on the temperature of the applied liquid. In the presented case the water was at the ambient temperature. If the temperature of the liquid differs from the ambient temperature, the peak of V_{out} can be as high as a few mV, as also demonstrated in the following (see Section 4.3).

2.3. Experiments with different fluids

The same experimental procedure was repeated for ethanol and silicone oil. In the same way, we introduced the drops of the liquids onto the central part of the diaphragm until the cumulative liquid stream covered the entire surface. During this time the output voltage V_{out} was measured continuously. The results obtained in the room's ambient conditions are presented in Fig. 3. It is evident that ethanol causes similar changes in V_{out} as water, while the sensor's response in the case of silicone oil showed only an instantaneous destabilization at the moment when the drop contacted the diaphragm. The main difference between the responses measured during the experiment with the water and the one with ethanol is in the shorter drying interval 5–6 (Fig. 2b), i.e., at the time when the narrow region at the edge of the diaphragm is still drying. Fig. 3 shows the sensor's response measured during the experiments with the drops of ethanol and silicone oil, which were dropped in the centre of the diaphragm and followed by small streams (of about 60 μl), which spread over the entire diaphragm and then slowly dried (in the case of volatile liquids). Notice, how-

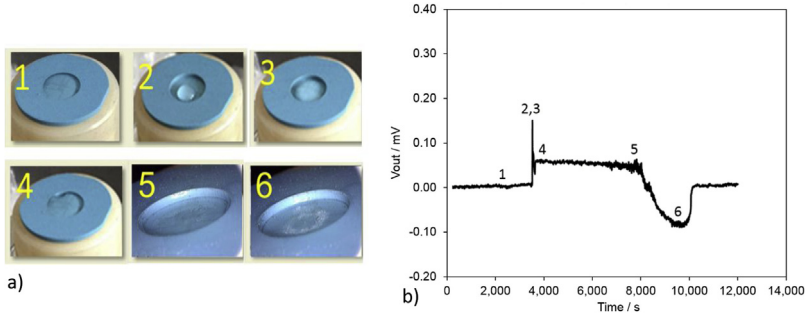

Fig. 2. a) Sensor structure in the observed situations: (1) the back side of the diaphragm, (2) one drop of water on the diaphragm, (3) accumulated three drops of water, (4) the film of water over the whole diaphragm, (5) the central part of diaphragm is already dried, (6) the narrow region at the edge of the diaphragm is still wet; b) Output voltage (V_{out}) measured at V_s = 5 V.

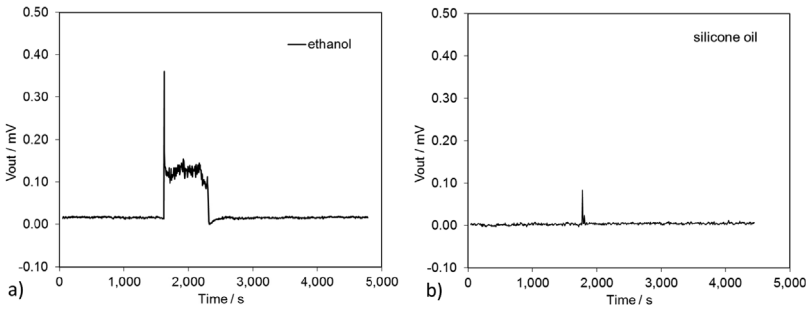

Fig. 3. Sensor's response to a) a drop of ethanol; b) a drop of silicone oil.

ever, that the wetting behaviour can change and, potentially, this can have an effect on the response.

The results can be interpreted as follows. The LTCC has closed pores so that the water or another fluid remains on the surface (and in the surface pores) of the diaphragm. A liquid evaporating from the surface has a cooling effect. When the drops of the liquid suddenly appear at certain locations on the diaphragm, they affect the temperature equilibrium of the system, which is continuously heated by the thick-film resistors. These dynamic changes are reflected in the functional response of the sensor. One drop falling on the centre of the membrane causes a distinct peak in the response. After applying enough drops, the liquid spreads over the whole of the diaphragm. This affects the temperature distribution and the response changes accordingly. As soon as the evaporating film of the liquid is selectively dried out from certain regions on the diaphragm's surface, the temperature in these regions starts rising again. In the case of the non-volatile liquid (silicone oil) V_{out} is quickly raised when the liquid touches the diaphragm (due to the heat conduction), and then immediately returns to its initial value. We assume this is because the small difference between the temperature of the drop and the central resistors (of less than 1 ° C) is very rapidly balanced and then there is no longer any temperature change, as in the case of cooling due to the evaporation of the liquid. In order to confirm the above interpretation and further examine the observed trends, we performed numerical simulations.

3. Numerical modelling

The thermal state observed in the above experiments is defined by the heat transfer, which is primarily due to the liquid that is evaporating from its surface. The general equation governing the heat transfer in fluids and solids [24] is given by (1),

$$\rho C_p \frac{\partial T}{\partial t} + \rho C_p u \cdot \nabla T = \nabla \cdot (k \nabla T) + Q \quad (1)$$

where ρ is the density, C_p is the heat capacity at constant pressure, k is the thermal conductivity, Q is the heat source (or sink) and u is the velocity field, which can be specified either by an analytical expression or a velocity field from a fluid-flow interface.

The outward heat flux from the boundary of the heated solid body can be expressed by:

$$n \cdot (-k \nabla T) = h\,(T - T_\infty) + \varepsilon \sigma\,(T^4 - T_\infty{}^4) \quad (2)$$

where n is the outward surface normal vector, h is the convection heat-transfer coefficient, σ is the Stefan-Boltzmann constant, ε is the emissivity of the surface and T_∞ is the ambient temperature far from the observed surface.

When the evaporating liquid is on the surface of the solid body, the heat transfer refers to the combination of molecular diffusion and fluid motion. In order to avoid any formulation of the vanishing fluid domain, we made several simplifying assumptions. Instead of calculating the dynamic fluid flows resulting from the evaporation we translated the problem to the analysis of a solid body exposed to forced cooling on its surface. The heat for the evaporation is absorbed from the fluid itself and the surroundings, and in the case of a very thin film of liquid, we can assume that the heat is transferred directly from the solid structure and neglect the liquid. In this way, we modelled the convective evaporation of the vanishing liquid domain by defining the forced convection on the diaphragm's surface. The convective heat-transfer coefficient depends on the properties of the fluid and the physical situation. These coefficients are normally obtained using empirically derived relationships, which have been found to work well in practice. We have roughly estimated it for our case in accordance with the data in the literature [14–16].

3.1. FE model

For solving the described heat-transfer problem we used the Comsol Multiphysics environment with the MEMS module having built-in interfaces for piezo-resistivity and heat-transfer problems. We followed the modelling strategy described in [13] and upgraded the model by adding the heat-transfer interface prescribed for modelling the heat transfer by conduction, convection and radiation.

Because of the high aspect ratio of the structure's geometry (the thickness of the thick films is 15–25 μm and the lateral dimensions are from a few to more than ten mm), a large number of elements is needed to adequately discretize the sensor's geometry. In order to keep the model's size manageable, the layout of the thick-film regions (resistors and conductor lines) was slightly streamlined. The resistors and conductor lines were assumed to be of the same thickness (20 μm). In a further simplification of the model's geometry, the approximately 25-μm-thick protective coating covering the conductor lines and the thick-film resistors R_5 and R_6 (Fig. 1) was omitted from the model. To describe the dynamics of the selective drying of the diaphragm's surface (which starts in the central part and extends towards the edge), we discretized the surface of the diaphragm in nine concentric rings, and for each region defined other time-dependent boundary conditions. The model geometry is shown in Fig. 4. The number of degrees of freedom for this model [25] is of the order of 10^6.

The material parameters specified for the domains of the LTCC, the conductor lines, the connection pads, and the thick-film resistors were the same as used in [13], only the temperature dependency of the thick-film resistors was updated for this case study. The electrical conductivity of the resistor material was defined as a piecewise linear function of the temperature with a linear temperature coefficient (TCR) of $70 \times 10^{-6}\,K^{-1}$ in the temperature range of interest (15–35 °C). This TCR value was taken from the experimental data for the DuPont 2041 resistors post-fired on the DuPont 951 substrates that were reported in [17]. The specific heat of the resistive material was assumed to be $600\,J\,kg^{-1}\,K^{-1}$.

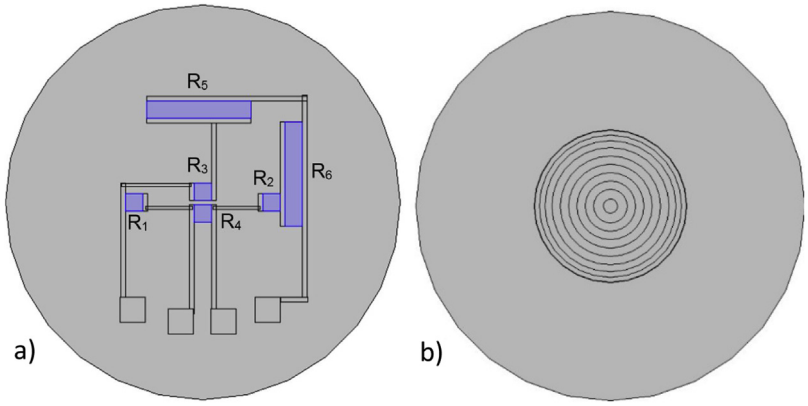

Fig. 4. Model geometry: a) Front view: Wheatstone bride with additional resistors R_5 and R_6 on the rigid ring around the diaphragm; b) Back side of the diaphragm discretized into 9 concentric regions, denoted as $ring_i$ (i = 1..9).

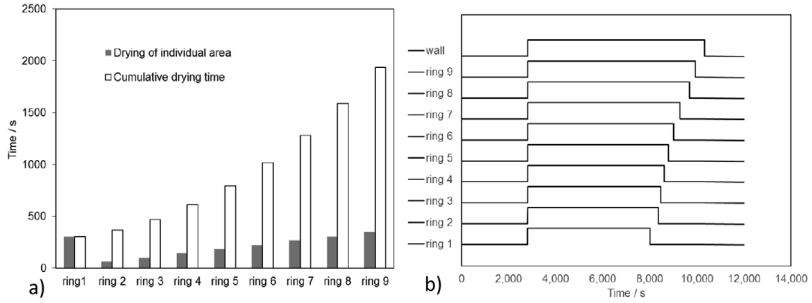

Fig. 5. a) Calculated time required for drying individual regions; b) Time intervals for drying the regions.

For the LTCC material, a thermal conductivity of 3 $Wm^{-1}\,K^{-1}$ and a specific heat of 729 J kg^{-1} K^{-1} were used.

The boundary conditions and loads were as follows. On the boundaries of the structure, which are never in contact with the water/liquid, natural convection is assumed, while at the boundaries of the wet surfaces, which are drying by evaporation, heat transfer is defined as forced convection. On the boundaries of the regions that are temporarily covered with the liquid (i.e., water), we defined the convection coefficient as a function of the time $h(t)$,

$$h(t) = \begin{cases} h_{01},\ t_2 < t < t_1 \\ h_{02},\ t_1 < t < t_2 \end{cases} \tag{3}$$

where h_{01} is the natural convection coefficient in air, h_{02} is the forced convection coefficient due to evaporation from the surface, t_1 is a time when the liquid is applied and t_2 is the time when the surface is again dry. According to the common data for the convective heat-transfer coefficients reported in [15,16], we specified h_{01} = 5 $Wm^{-2}\,K^{-1}$ and h_{02} = 3000 $Wm^{-2}\,K^{-1}$.

The drops/stream of water on the diaphragm was considered as follows. At the moment when the first drop of water (at the ambient temperature of the room) comes into contact with the surface of the diaphragm, which is heated by resistors, the heat transfer from the diaphragm to the drop is primarily by conduction. This situation was modelled by defining a small cylindrical domain for the drop of liquid on the diaphragm. On the upper surface of the drop domain, the initial temperature of the drop was defined (T_0 = 25 °C). The conduction of heat between the drop and the diaphragm has the dominant effect on the response of the sensor structure in the short initial time interval (t_0, t_1), during which we presume that the temperature of the drop and the ceramic below it are balanced. After this period the forced convection prevails. We modelled such a situation by specifying the thermal conductivity of the drop as a function of time $k_d(t)$,

$$k_d(t) = \begin{cases} k_1,\ t_0 < t < t_1 \\ k_2,\ t_1 < t < t_2 \\ k_3,\ t < t_0 \,and\, t_2 < t \end{cases} \tag{4}$$

where t_0 corresponds to the moment when the drop falls onto the diaphragm's surface, t_1 designates the moment when the forced convection (evaporation) prevails and t_2 is when the drop is dried. k_1 is an assumed high value of the thermal conductivity attributed to the drop domain at the moment when the drop comes into contact with the diaphragm; k_2 is the thermal conductivity of the liquid (attributed to the drop in the period when the heat transfer by conduction is taking place); k_3 is a fictional low thermal conductivity illustrating a thermal barrier preventing the conduction of heat before the drop is dispensed on the diaphragm and after the diaphragm is dried (the liquid is completely dried out). For k_1, k_2 and k_3 we assumed $10e^2$ $Wm^{-1}\,K^{-1}$, 0.6 $Wm^{-1}\,K^{-1}$ and $10e^{-6}$ $Wm^{-1}\,K^{-1}$, respectively.

The situation when the water covering the diaphragm is drying is modelled by the time-dependent boundary conditions on individual segments of the diaphragm's surface. For this we defined the heat-exchange coefficients on the outer surface of nine concentric ring-segments ($ring_i$, i = 1..9) as a function of time (5), where t_{1i} and t_{2i} define the specific time intervals for each individual area (ring i).

$$h_{ring\,i}(t) = \begin{cases} h_{01},\ t < t_{1i}\, and\, t_{2i} < t \\ h_{02},\ t_{1i} < t < t_{2i} \end{cases},\ i = 1, 2, .., 9 \tag{5}$$

In other words, the function $h_{ringi}(t)$ determines the time intervals during which the separated ring is cooled by natural convection (coefficient h_{01}) or forced convection (coefficient h_{02}). The time

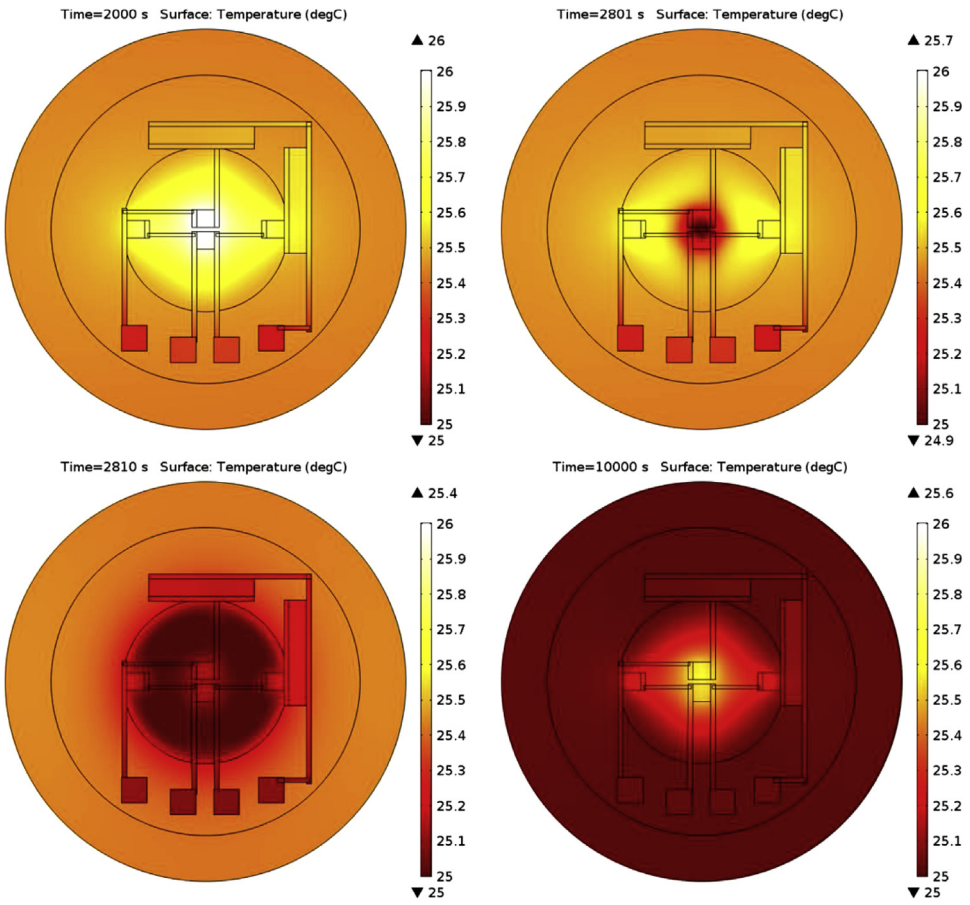

Fig. 6. Simulated temperature distribution in the sensor structure at: (a) t = 2000s (warmed up and stabilised), (b) t = 2801s (1 s after the first drop of water touched the diaphragm), (c) t = 2810s (the diaphragm is covered with a film of water), (d) t = 10,000 s (the central part of the diaphragm has dried out).

intervals needed for drying the appropriate mass of water (Fig. 5) were calculated from the experimental data [25]. Fig. 5a shows the time required for drying the diaphragm covered with a 15-μm thin film of water, which was estimated by assuming that drying a drop of 8 ml takes about 400 s and that all the rings dry with a constant speed, independently of the local temperature of the diaphragm [26]. Notice, however, that the assumed drying time for individual rings (time t_{1i}) represents only a rough approximation to the real situation observed during the experiment presented in Fig. 2. Fig. 5b shows the time intervals defined for drying the ring regions on the diaphragm's surface ($ring_i$, i=1..9) and the region reg_{10} on the wall of the LTCC structure at the edge of the diaphragm.

4. Simulation results

4.1. Experiment with water

We simulated the response of the sensor for the case of the ideally balanced Wheatstone bridge (R_1—R_4 = 10 kΩ, R_5=R_6 = 0) and for the slightly unbalanced bridge, with the resistors R_5=R_6 = 2 kΩ. The ambient temperature and the initial temperature of the water were set to 25 °C. The temperature distribution at some characteristic moments is shown in Fig. 6.

The simulations also showed that the Joule heating of the resistors R_5 and R_6, located on the rigid substrate that is much thicker than the diaphragm, does not change significantly the temperature gradient that determines the sensor's response. In any case, the temperature gradient remains within one degree Celsius. The changes in the temperature and the resistance of R_1–R_4 during the experiment with water are shown in Fig. 7.

The simulated response V_{out} is presented in Fig. 8a. Notice that this graph includes the initial 50–100 s warm-up period, which is not captured in Fig. 2b. We also checked the effect of the protective coating and the comparison shows that it does not significantly influence the observed trends, as can be seen in Fig. 8b.

The specific intervals of the simulated response can be summarized as follows:

- The warm-up period (interval: t < 100 s), which mainly depends on the TCR;
- The stabilized response during the unloaded normal operation (interval: 100 s < t < 2800s);
- The peak corresponding to the rise in the output voltage after the drop of water at ambient temperature (25 °C) touches the diaphragm at t = 2800s;
- The water is spread over the entire surface of the diaphragm 2810s < t < 8400 s;
- Drying of the central part of the diaphragm (interval: 8400 s < t < 10,000 s),
- Drying of the narrow region at the border of the diaphragm (interval: 10,000 s < t < 11,000 s),
- Stabilized operation of the completely dry structure.

However, for volatile liquids, the magnitude of the effect can vary with parameters such as the volatility and the latent heat of evaporation.

The matching of the simulated characteristics with the typical measured characteristic (Fig. 1) confirmed the proposed modelling

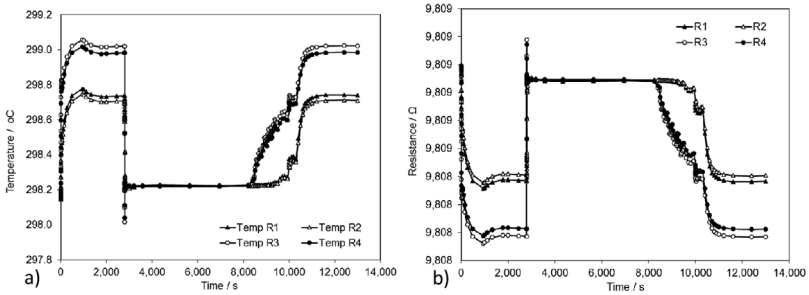

Fig. 7. (a) Simulated average temperature of the thick-film resistors during the experiment with water for the case of the slightly unbalanced bridge ($R_1 = R_2 = R_3 = R_4 = 10$ KΩ and $R_5 = R_6 = 2$ KΩ); (b) Simulated changes in the resistance of the bridge resistors.

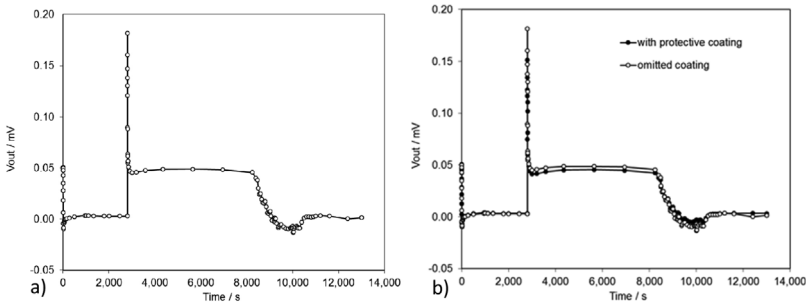

Fig. 8. a) Simulated response during the experiment with drops of water presented in Fig. 2; b) The response with and without the protective coating.

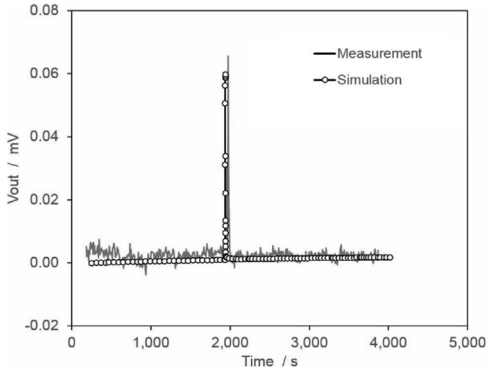

Fig. 9. Simulated and measured responses of the test structure during an experimental procedure with a drop of silicone oil, which spreads over the whole surface of the diaphragm.

strategy. Nonetheless, we carried out a supplementary validation using experiments with non-volatile liquids and a drop of hot water, as described in the following paragraphs.

4.2. Experiment with silicone oil

For the analysis of the sensor's response in the case when silicone-oil drops are applied (the measurements in Fig. 3b) we modified the model parameters appropriately. Because the silicone oil does not vaporize, the coefficient of the forced convective evaporation was replaced by the natural convection coefficient (i.e., $h_{02} = h_{01} = 5\ W/m^{-2}\ K^{-1}$). The simulation results are in good agreement with the measurement results (Fig. 9). This matching further validates the model.

4.3. Variation of the model parameters

Exploitation of the discussed phenomena offers new possibilities for applications of the LTCC sensor structure, such as the detection of drops at certain locations on the sensor's surface. LTCC is an inherently suitable material because it has a relatively low thermal conductivity and consequently a higher thermal gradient in the diaphragm. In this respect, we were interested in the response of the sensor if it was made from other materials and for an experiment under different conditions. Since the material parameters used in the above-described model (Section 4.1) were taken from the literature (where they correspond to other situations/structures) and the heat-transfer coefficients defined on the surface were fictional, we performed further analyses to assess how the uncertainty (variations) of the model's parameters affect the simulation results. In this context, we carried out further analyses of the experiment with water drops for different material parameters, as follows.

Initially, in the model, we specified for the resistive material the temperature coefficient (TCR) calculated from the experimental data [17]. However, this corresponds to another test structure (with a thicker substrate) and was measured for another operating condition. Consequently, in our case we can expect that the actual TCR will deviate slightly from this value. Instead of performing a parametric analysis to assess the influence of these small deviations, we considered two different thick-film resistor materials, namely DuPont 2041 and ESL 3414B, which have temperature coefficients of resistance equal to $-60 \times 10^{-6}\ K^{-1}$ and $-330 \times 10^{-6}\ K^{-1}$, respectively [18]. The difference in the simulated responses is obvious (Fig. 10). The replacement of the thick-film resistor material results in a non-negligible change in V_{out}. The effect is more pronounced for the resistors with higher TCR.

On the other hand, the effect would be much less pronounced for sensor structures made of materials with a higher thermal conductivity (e.g., Al_2O_3 ceramic, which has a 10-times-higher coefficient of thermal conductivity than LTCC). The simulation results obtained for the sensor made of Al_2O_3 ceramic and the LTCC-based sensor are presented in Fig. 11. The simulated V_{out} shows a noticeable peak at the moment when the drop of water touches the diaphragm, similar to the response of the LTCC sensor measured during the experiment with silicone oil. Due to the high thermal conductivity of the Al_2O_3 diaphragm, the local cooling effect of the water is nearly negligible.

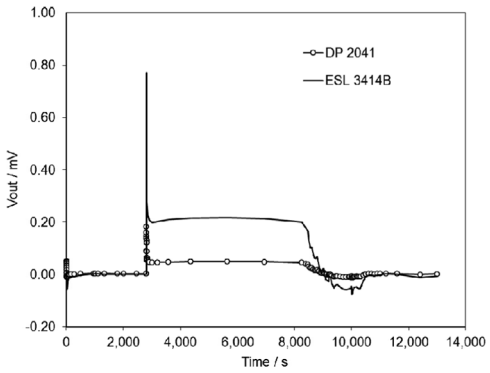

Fig. 10. Results of the simulation of the experiment with drops of water that spilled over the diaphragm and then dried, carried out for two different resistor materials (DuPont 2041 and ESL 3414B).

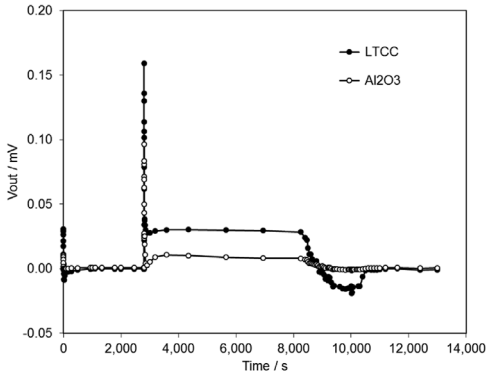

Fig. 11. Simulated response of an Al_2O_3-based sensor compared to the response of an LTCC sensor.

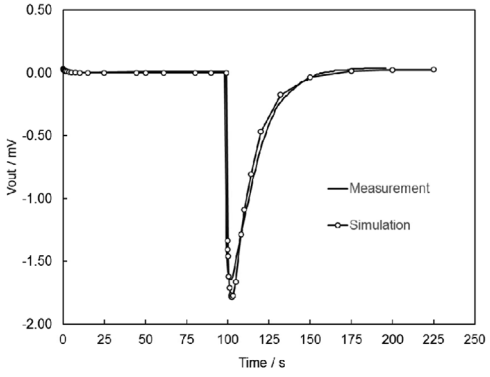

Fig. 12. Measured and simulated responses of the sensing structure to the drops of hot water (50 °C) dispensed onto the diaphragm under ambient room conditions.

In the subsequent numerical experiment, we looked at the case when a drop of water that is not at room temperature falls on the diaphragm. We performed the analysis only for a short period, starting when the drop of water touches the diaphragm, until the temperature of the system is balanced, and therefore appropriately updated the model. The simulated response to the droplet of water at 50 °C was a good match with the measurements (Fig. 12), which also validates the model for this specific situation.

5. Possible exploitations

The scientific literature and different professional/engineering forums often mention the need to detect drops or small streams of liquids (quantities in the range of a few microlitres to several tens of microlitres) [19–23,26]. The problem of drop detection can be solved by using different detection devices based on different physical principles (electrostatic, capacitive, magnetic, acoustic and optical detection devices). An example of the optical drop-detection device/method is a sensor that uses a high-intensity, light-emitting component and a light-detecting device (a photodiode), positioned in such way that it receives the light scattered and reflected from drops of fluid [20]. In such a device, the photodetector is connected to a controller that uses the received information to determine the presence and the number of drops. In [21] a new approach based on the 3ω method, typically used to measure the thermal properties of a small volume of sample, was suggested for the detection of droplets and the difference in its composition (contents). In [22] an analytical detector based on a liquid-drop resistor-capacitor (RC) filter is presented, which can be used to detect dielectrically different species dissolved in a liquid (e.g., water and alcohol). In [23] the authors describe a method for analysing liquid biological media based on the photometry of the biological liquid drops.

The experimental and numerical results presented in Section 4 suggest a possible exploitation of the thermal effect in the LTCC Wheatstone-bridge sensing structure in new applications. Due to the good mechanical and chemical stability of LTCC ceramics, such structures are appropriate for applications in which direct contacts with different liquids are essential. An important advantage is that the liquids can be electrically conductive or non-conductive, coloured or transparent, volatile or non-volatile.

5.1. Detecting drops and small streams of liquids

Based on the above-presented results, LTCC sensors might be suitable for the real-time detection of liquid droplets and can even provide some additional information about the liquid. The LTCC structure with the temperature-dependent thick-film resistors in a Wheatstone bridge is simple and very sensitive to any change in the temperature gradient. Moreover, different design/layout options are possible. The liquid-drop detection is based on a simple measurement of the bridge's output voltage, which is very sensitive to any temperature imbalance of the bridge's resistors and so works well even for transparent liquids. There is no need to use complex electronics for the signal processing. It also enables the detection of drops of transparent liquids, which can be problematic for detection when using an optical solution. It is important to note that the sensor's response (which follows the changes in temperature of the sensing resistors due to the applied liquid drops), greatly depends on the temperature of the liquid and the ambient conditions. In Section 2.2 we discussed the response of the sensor to the presence of liquids, which before the application were kept at room temperature. In such cases, the drop of liquid dispensed in the centre of the diaphragm causes a lowering of the temperature of the resistors located in the central region of the diaphragm by less than one degree Celsius. This leads to V_{out} increasing by a few tenths of a mV. Taking into account the relatively good stability of the output signal, changes in V_{out} of a few hundred μV can be sufficient to detect the dispensed droplets (under constant ambient conditions and a stable V_s of 5 V, ΔV_{out} is typically less than 10 μV/hour and $\Delta V_{s\,rms} < 6e^{-5}$). However, in the case of a greater deviation of the temperature of the liquid from the ambient temperature, the response of V_{out} to the dispensed liquid drops can be as high as a few mV (Fig. 12). In this way, it is also possible to obtain information about the temperature of the drops.

5.2. Identifying different liquids

The experiments with different liquids showed that the response of the sensing structure to the drop or some small stream of liquid depends on the ambient conditions (temperature, rela-

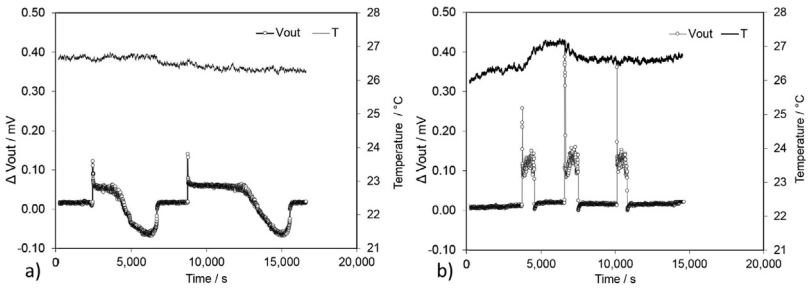

Fig. 13. V_{out} measured continuously during successive attempts with drops of liquid that quickly spread over the entire surface of the diaphragm and then dried for (a) deionized water; (b) ethanol.

tive humidity, air movement, which affect the evaporation of the liquid), the amount of liquid and its properties. Under constant ambient conditions, the response is repeatable and unique for individual liquids. An example of such measurements is presented in Fig. 13, which shows the sensor's responses to a few successive drops of ionized water and ethanol. This experiment demonstrates that the use of the LTCC-based sensing structure under controlled conditions and with precise dosing of the drops can provide information about the applied liquid. Moreover, it is possible to build an extended sensor system with two sensing structures, which might give information about both the environmental conditions and the liquid properties. Such a system could be used to analyze the composition of liquids.

5.3. Further considerations

Depending on the target application the sensor device can be optimized and calibrated either for accurate measurements of pressure or to give appropriate responses to other changes in the environment (e.g., the detection of volatile liquids). Notice, however, that the discussed thermal phenomenon has been observed in the absence of pressure loads so that for the exploitation of further functionalities the appropriate conditions should be enabled. Alternatively, a system of two identical sensors where one of them is protected from contact with the liquid might be a solution for differential measurements of the thermal effect. Hence, possible applications can be regarded as an add-on option for the detection/identification of liquid drops.

When designing a device for the detection of volatile liquids, or for an analysis of the composition of the liquid droplets, the use of thick-film thermistors (PTC or NTC) could be an interesting solution. Several studies [27–29] showed promising characteristics for some commercial thick-film thermistor material processed on LTCC. The replacement of the strain-sensitive resistors in the Wheatstone bridge with thermistors, which have much more pronounced temperature dependency, would greatly improve the functional resolution.

6. Conclusions

We investigated the effects of liquid droplets on the response of a thick-film piezoresistive LTCC pressure sensor in a Wheatstone-bridge configuration and the possible exploitation of the LTCC sensor structure.

Experiments showed that the presence of volatile liquids on the diaphragm greatly influences the sensor's response. We modelled the sensor in such conditions using the Comsol Multiphysics environment with the MEMS module, which has built-in interfaces for piezo-resistivity and heat-transfer problems. The FE analyses confirmed our assumptions that the specific dynamic response observed during the experiment with droplets of volatile liquids on the diaphragm comes mainly from the dynamic changes in the temperature distribution due to the Joule heating of the thick-film resistors and the local cooling caused by the evaporation of the liquid covering the sensing structure. For validation purposes, supplementary experiments with non-volatile silicone oil and a drop of hot water were carried out.

The simulations also showed that due to the lower thermal conductivity, LTCC can be appropriate for the creation of functional structures aimed at the detection of dynamic changes in the local temperature distribution. It is important to note that such effects cannot be observed in the case of sensing structures made of materials with higher thermal conductivities (e.g., Al_2O_3 ceramic, which has a 10-times-higher coefficient of thermal conduction).

The thermal phenomenon can be exploited in monitoring environmental conditions, the detection of drops and small streams of liquids, the identification of different liquids and other applications. Depending on the target application, the sensor device can be optimized. To increase the sensitivity, the implementation of thick-film thermistors (PTC or NTC) could be a good solution.

In this paper we have highlighted the possibility of exploiting the thermal effects in LTCC-based Wheatstone-bridge sensor configurations. The developed FE model provides a means for predicting the structure's response in specific situations. Further improvements for special situations would also be possible when applied to real, practical examples.

Acknowledgement

The authors acknowledge the financial support from the Slovenian research agency (research core funding No. P2-0098).

References

[1] M.R. Gongora-Rubio, P. Espinoza-Vallejos, L. Sola-Laguna, J.J. Santiago-Aviles, Overview of low temperature co-fired ceramics tape technology for meso-system technology (MsST), Sens. Actuators A Phys. 89 (2001) 222–241.
[2] G.J. Radosavljević, L.D. Zivanov, W. Smetana, A.M. Marić, M. Unger, L.F. Nađ, A Wireless Embedded Resonant Pressure Sensor Fabricated in the Standard LTCC Technology, IEEE Sens. J. 9 (12) (2009) 1956–1962.
[3] D. Jurków, T. Maeder, A. Dąbrowski, M.S. Zarnik, D. Belavič, H. Bartsch, J. Müller, Overview on low temperature Co-fired ceramic sensors, Sens. Actuators A 233 (2015) 125–146.
[4] Y. Fournier, T. Maeder, G. Boutinard-Rouelle, A. Barras, N. Craquelin, P. Ryser, Integrated LTCC Pressure/Flow/Temperature multisensor for compressed air diagnostics, Sensors 10 (2010) 11156–11173.
[5] U. Partsch, C. Lenz, S. Ziesche, C. Lohrberg, H. Neubert, T. Maeder, J. Microelectron, Electron. Compon. Mater 42 (4) (2012) 260–271.
[6] F. Rettig, R. Moos, Ceramic meso hot-plates for gas sensors, Sens. Actuators B 103 (2004) 91–97.
[7] S. Achmann, M. Hämmerle, J. Kita, R. Moos, Miniaturized low temperature co-fired ceramics (LTCC) biosensor for amperometric gas sensing, Sens. Actuators B 135 (2008) 89–95.
[8] H. Bartsch, C. Rensch, M. Fischer, A. Schober, M. Hoffmann, J. Müller, Thick film flow sensor for biological microsystems, Sens. Actuators A 160 (2010) 109–115.
[9] L.J. Golonka, K. Malecha, LTCC fluidic microsystems, J. Microelectron. Electron. Compon. Mater 42 (2012) 225–233.
[10] W. Missal, J. Kita, W. Eberhard, F. Gora, A. Kipka, T. Bartnitzek, F. Bechtold, D. Schabbel, B. Pawlowski, R. Moos, Miniaturized ceramic differential scanning

calorimeter with integrated oven and crucible in LTCC technology, Sens. Actuators A Phys. 172 (2011) 21–26.
[11] M.S. Zarnik, D. Belavic, Study of LTCC-based pressure sensors in water, Sens. Actuators A Phys. 220 (2014) 45–52.
[12] M.S. Zarnik, F. Novak, Effect of condensing environments on characteristics of piezoresistive ceramic pressure sensors, Sens. Actuators A 267 (2017) 385–392.
[13] M.S. Zarnik, D. Belavic, F. Novak, The Impact of Housing on the Characteristics of Ceramic Pressure Sensors — An Issue of Design for Manufacturability, Sensors 15 (2015) 31453–31463.
[14] Greg F. Naterer, Heat Transfer in Single and Multiphase Systems, CRC Press LLC, 2003.
[15] The Engineering Toolbox, 2019, Available online: (accessed 14. 02. 2018) http://www.engineeringtoolbox.com/convective-heat-transfer-d_430.html.
[16] H.D. Baehr, K. Stephan, Heat and Mass Transfer, Second Revised Edition, Springer-Verlag, Berlin Heidelberg, 2006.
[17] M. Hrovat, D. Belavič, M.S. Zarnik, M. Jerlah, J. Holc, J. Cilenšek, S. Drnovšek, M. Kosec, Thick film sensing elements on LTCC structures, J. Microelectron. Electron. Compon. Mater. 41 (2011) 279–283.
[18] D. Belavic, M. Hrovat, J. Holc, M.S. Zarnik, M. Kosec, M. Pavlin, The application of thick-film technology in C-MEMS, J. Electroceramics 19 (4) (2007) 363–368.
[19] Parallax Discussion Forum, 2019 (accessed on March 2009) http://forums.parallax.com/discussion/111565/sensor-to-detect-drops-of-liquid.
[20] K. Ward, A. Govyadinov, Patent US 20150116406 A1.
[21] Y. Namwoo, K. Dongsik, P. Jaesung, In situ micro droplet typing system using 3ω method, International Conference on Miniaturized Systems for Chemistry and Life Sciences (2010) 3–7.
[22] Y.S. Nanayakkara, D.W. Armstrong, A liquid drop RC filter apparatus for detection, Anal. Bioanal. Chem. 401 (9) (2011) 2669–2678 (doi: 10.1007/s00216-011-5426-0) http://link.springer.com/article/10.1007/s00216-011-5426-0.
[23] A. Aristov, E. Nosova, N. Nefedova, Method of droplet samples photometry for the analysis of biological liquids, in: International Siberian Conference on Control and Communications (SIBCON), 2016.
[24] COMSOL Multiphysics® Reference Manual (version 4.4), 2019.
[25] What does degrees of freedom (DOFs) mean in COMSOL Multiphysics? 2019 https://www.comsol.com/support/knowledgebase/875/.
[26] H. Gelderblom, Fluid Flow in Drying Drops, Physics of Fluids (ISBN: 978-90-365-3525-0) Available online, University of Twente, 2013 https://research.utwente.nl/en/publications/fluid-flow-in-drying-drops.
[27] M. Hrovat, D. Belavič, J. Kita, J. Holc, S. Drnovšek, J. Cilenšek, M. Kosec, A. Dziedzic, L.J. Golonka, Thick-film strain and temperature sensors on LTCC substrates Microelectron. Int. 23 (2006) 33–41, http://dx.doi.org/10.1108/13565360610680749.
[28] H. Birol, T. Maeder, C. Jacq, P. Ryser, Effects of firing conditions on thick-film PTC thermistor characteristics in LTCC technology, Proceedings, Ceramic Interconnect Technology Conference, IMAPS (2004) 106–109.
[29] J. Zhong, H.H. Bau, Thick-film thermistors printed on LTCC tapes, Am. Ceram. Soc. Bull. 80 (2001) 39–42.

Biographies

Marina Santo Zarnik received an M.Sc. degree in Computer Science and a PhD in Electrical Engineering from the University of Ljubljana, Slovenia, in 1993 and 1998, respectively. Her research field covers different areas of ceramic microsystems and sensors. Her main interest comprises experimental characterization and finite-element modelling of thick-film functional structures and ceramic electromechanical systems.

Franc Novak gained the BSc, MSc, and PhD degrees in electrical engineering from the University in Ljubljana in 1975, 1977, and 1988, respectively. Since 1975 he has been with the Jožef Stefan Institute, where he was head of Computer Systems Department (1994–2014). Since 2010 he is also full prof. at Faculty of Electrical Engineering and Computer Science, University of Maribor. His research interests are in the areas of electronic design and test and fault-tolerant computing.

Gregor Papa received the PhD in Electrical Engineering from the University of Ljubljana, Slovenia, in 2002. He is a Senior researcher and a Head of Computer Systems Department at the Jožef Stefan Institute, and an Associate Professor at the Jožef Stefan International Postgraduate School. His research interests include metaheuristic optimization methods and hardware implementations of high-complexity algorithms.